Loss of a highly conserved sterile alpha motif domain gene (*WEEP*) results in pendulous branch growth in peach trees

Courtney A. Hollender[a,b], Thierry Pascal[c], Amy Tabb[a], Toto Hadiarto[d], Chinnathambi Srinivasan[a], Wanpeng Wang[e], Zhongchi Liu[e], Ralph Scorza[a], and Chris Dardick[a,1]

[a]Appalachian Fruit Research Station, Agricultural Research Service, US Department of Agriculture, Kearneysville, WV 25430; [b]Department of Horticulture, College of Agriculture and Natural Resources, Michigan State University, East Lansing, MI 48824; [c]Unité Génétique et Amélioration de Fruits et Légumes, Institut National de la Recherche Agronomique, 84140 Montfavet, France; [d]Indonesian Center for Agricultural Biotechnology and Genetic Resources Research and Development (BB Biogen), Bogor, Indonesia; and [e]Department of Cell Biology and Molecular Genetics, College of Mathematics and Natural Sciences, University of Maryland, College Park, MD 20742

Edited by Mark Estelle, University of California, San Diego, La Jolla, CA, and approved February 23, 2018 (received for review March 27, 2017)

Plant shoots typically grow upward in opposition to the pull of gravity. However, exceptions exist throughout the plant kingdom. Most conspicuous are trees with weeping or pendulous branches. While such trees have long been cultivated and appreciated for their ornamental value, the molecular basis behind the weeping habit is not known. Here, we characterized a weeping tree phenotype in *Prunus persica* (peach) and identified the underlying genetic mutation using a genomic sequencing approach. Weeping peach tree shoots exhibited a downward elliptical growth pattern and did not exhibit an upward bending in response to 90° reorientation. The causative allele was found to be an uncharacterized gene, *Ppa013325*, having a 1.8-Kb deletion spanning the 5′ end. This gene, dubbed *WEEP*, was predominantly expressed in phloem tissues and encodes a highly conserved 129-amino acid protein containing a sterile alpha motif (SAM) domain. Silencing WEEP in the related tree species *Prunus domestica* (plum) resulted in more outward, downward, and wandering shoot orientations compared to standard trees, supporting a role for WEEP in directing lateral shoot growth in trees. This previously unknown regulator of branch orientation, which may also be a regulator of gravity perception or response, provides insights into our understanding of how tree branches grow in opposition to gravity and could serve as a critical target for manipulating tree architecture for improved tree shape in agricultural and horticulture applications.

tree architecture | weeping | SAM domain | peach | gravitropism

Trees have a tremendous degree of architectural plasticity, allowing them to adopt a broad range of shapes and growth habits. This morphological diversity is a consequence of fine-tuned genetic and environmental interactions that allow them to compete for light in crowded conditions. For example, responses to light and gravity signals are hierarchically regulated such that upper branches often respond differently than lower branches—a phenomenon referred to as apical control (1). Currently, little is known about the molecular mechanisms underlying such developmental phenomena, in part due to the general intractability of trees for genetic studies. Over the past few years, a handful of reports have begun to reveal insights into the determination of growth habits using mutant trees that display distinct architectural phenotypes. Dwarfism in peach (*Prunus persica*) marked by shortened internodes was found to be caused by a nonsense mutation in a gene encoding a gibberellic acid (GA) receptor, GA INSENSITIVE DWARF 1C (2). ARBORKNOX 2 was found to be required for normal gravibending responses in poplar mediated by endodermal and secondary phloem cells (3). In apple, a retrotransposon insertion was found to be associated with the columnar growth habit possibly via up-regulation of an adjacent 2OG-Fe(II) oxygenase (4–6). Likewise, a mutation in the Tiller Angle Control 1 (*TAC1*) gene was shown to cause the pillar growth phenotype in peach trees (7). Mutations in *TAC1* also produced similar vertical growth phenotypes in *Arabidopsis*, rice, and maize, suggesting a high degree of functional conservation (7–9). *TAC1* was found to be a member of a small family that includes *LAZY1* and DEEPER ROOTING 1 (*DRO1*), two genes that also contribute to plant architecture (10–16). *LAZY1* mutations in *Arabidopsis*, rice, and maize exhibited horizontally oriented lateral shoots or tillers via reduced lateral auxin transport (11–14). Likewise, loss of *DRO1* resulted in horizontal lateral root growth in *Arabidopsis* and rice, while overexpression led to narrow root angles (15, 16). Collectively, these studies show that changes to tree architecture can be caused by distinct and often functionally conserved genetic pathways.

Trees with weeping branch architectures are objects of beauty that have been prized for centuries. Although not typically found in nature, such trees have been selected and propagated through cultivation for their ornamental appeal. Very few studies have characterized the genetics or physiology of weeping tree architectures, although these phenotypes have generally been

Significance

Trees' branches grow against the pull of gravity and toward light. Although gravity and light perception have been studied in model species, much is unknown about how trees detect and respond to these signals. Here, we report the identification of a gene (*WEEP*) that controls lateral branch orientations and is directly or indirectly required for gravity responses in trees. Loss or reduction of WEEP expression produced branches that grow outward and downward and did not exhibit normal gravitropism responses when displaced. WEEP is conserved throughout the plant kingdom and may be involved in gravity perception. WEEP may also be a valuable target for breeding or engineering trees with improved shapes for agricultural and landscaping applications.

Author contributions: C.A.H., A.T., and C.D. designed research; C.A.H., T.P., A.T., T.H., and C.S. performed research; C.A.H., A.T., C.S., W.W., Z.L., and R.S. contributed new reagents/analytic tools; C.A.H., T.P., A.T., and C.D. analyzed data; and C.A.H. and C.D. wrote the paper.

The authors declare no conflict of interest.

This article is a PNAS Direct Submission.

Published under the PNAS license.

The RNAseq data reported in this paper have been deposited in the Gene Expression Omnibus (GEO) database, https://www.ncbi.nlm.nih.gov/geo (accession no. GSE112080). The WEEP nucleotide sequence has been deposited in National Center for Biotechnology Information database (accession no. MH078037).

[1]To whom correspondence should be addressed. Email: chris.dardick@ars.usda.gov.

This article contains supporting information online at www.pnas.org/lookup/suppl/doi:10.1073/pnas.1704515115/-/DCSupplemental.

Published online April 30, 2018.

Downloaded at Palestinian Territory, occupied on December 9, 2021

www.manaraa.com

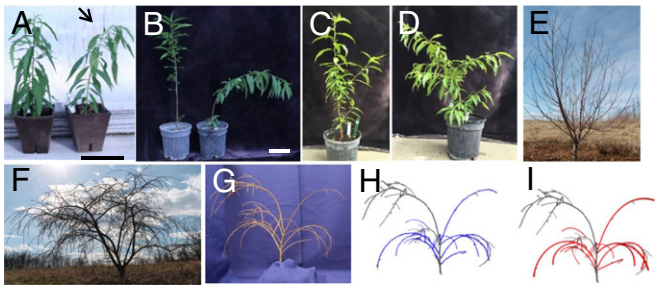

Fig. 1. Weeping peach tree branches arc and grow downward. (*A*) Young standard (*Left*) and weeping (*Right*) seedlings. Arrow indicates mild arcing. (*B*) Approximately 1-y-old standard (*Left*) and weeping (*Right*) trees. (*C* and *D*) Approximately 2-y-old standard (*C*) and weeping (*D*) potted trees. (*E* and *F*) Mature standard (*E*) and weeping (*F*) peach trees in the field. (*G*) The section of a field-grown weeping tree that was used for shape analysis. (*H* and *I*) A 3D reconstruction of the weeping shape. Gray regions represent branches that could not be evaluated. In *H*, elliptical branches are highlighted in blue. In *F*, elliptical branch models calculated from *I* are superimposed on the tree showing the model fit to the actual structure. (Scale bars in *A* and *B*: 4 in.)

attributed to a lack of branch structural integrity and insufficient tensile strength to support vertical branch orientations. Charles Darwin first detailed a handful of weeping traits in trees as examples of capricious inheritance due to their variable heredity (17). Since that time, weeping architectures in several tree species have been shown to segregate as single gene traits. A weeping phenotype in apple has been linked to a single dominant locus, while two distinct eastern redbud weeping phenotypes have been linked to recessive loci, and weeping phenotypes in chestnut have been linked to both recessive and dominant loci (18–22). Weeping in Japanese apricot (*Prunus mume*) was shown to be recessive and mapped to a region on linkage group 7 (23). To date, no causative alleles for weeping tree traits have been reported. Aberrant GA hormone concentrations and localization have been reported for a few weeping tree phenotypes, but the underlying significance of the observed differences remains unknown (24–28).

The genetics of weeping in peach trees has been studied for the last couple of decades due to its ornamental appeal and potential use in novel fruit tree production systems (29–32). Peach weeping was shown to segregate as a recessive locus and was named *pl* (short for pleureur, the French word for weeping) (29, 31–33). Studies by Werner and Chaparro (30) found that the "pillar" peach phenotype, caused by the *TAC1* mutation, was epistatic to the peach *pl* (weeping) locus (7, 30). Trees homozygous for both recessive traits displayed the pillar growth habit, while trees heterozygous for pillar and homozygous for weeping had a distinct phenotype called "archer," whereby the shoots grew on a slightly outward, curving trajectory that was intermediate to weeping (30). The genetic interaction between pillar and weeping suggests that similar mechanisms may be responsible for these growth types. Using random amplified polymorphic DNA markers, *pl* was positioned to linkage group 2 of an early peach genetic map; however, to our knowledge, this linkage map has not been oriented to the peach genome sequence (34).

Here, we used a mapping-by-sequencing strategy to identify *pl* as a mutation of a highly conserved but uncharacterized gene dubbed *WEEP*. This recessive mutant allele promotes downward elliptical branch growth and may be required for normal gravitropic responses. A transgenic approach was used to verify its function in *Prunus domestica* (plum), a related tree species that is amenable to transformation. Transcriptomic analyses suggested that WEEP is involved in cell wall reorganization and elongation. This work provides insights into the molecular basis of weeping architecture in trees.

Results

Phenotyping and Structural Analysis of Weeping Peach Trees. When germinated from seeds, the primary shoot tips of weeping trees initially grew upward, but often exhibited a mild downward arcing phenotype after the shoots reached ~20 cm in height (Fig. 1*A*). By the end of their first year of growth, some trees exhibited predominantly downward growth (Fig. 1*B*), while other trees exhibited a milder arcing phenotype (Fig. 1 *C* and *D*). As the weeping trees continued to grow and mature, reiterating arcing branch phenotypes became more apparent (Fig. 1 *E*–*G*). After a shoot committed to downward growth, a new shoot would typically grow from the peak of that branch and repeated the same growth pattern (Fig. 1 *F* and *G*).

To further evaluate this arcing branch orientation, 63 images of a representative weeping tree were taken at calibrated positions and processed with computer software to generate a 3D reconstruction (Fig. 1 *G*–*I*). Reconstructed branches were analyzed for fit with standard curvature models including a parabola, hyperbola, ellipse, and circle. The majority of branches (14 of 16) were found to have an elliptical shape marked by antipodal focal points that produced a major and minor axis (Fig. 1*I*). The parameters of the calculated weep branch ellipses are shown in Table S1. Superimposed elliptical models calculated for each branch showed a tight correlation with the branch reconstructions (Fig. 1*I*). The minimum curvature, which represents the flattest side of the ellipse, had a mean of 0.716 and SD of 0.1492, confirming a high degree of uniformity in the degree and manner of arc among weeping tree branches.

Weeping peach shoots (including the tips) were rigid and did not appear to have compromised structural integrity. This coupled with the finding that shoot tip arcing was visible upon the initial emergence of lateral shoots led us to hypothesize that weeping peach trees may lack or have altered gravity responses as opposed to reduced mechanical strength. Three 1-y-old standard and three 1-y-old weeping peach saplings were gravistimulated by 90° reorientation ~1 mo after emerging from dormancy (Fig. 2 *A*–*G* and Fig. S1*A*). Within 20 d, the standard peach trees exhibited classic gravitropic responses, including a partial upward lifting of the stem and upward growth of primary shoots (although this response was milder than gravitropic responses observed in other species) (Fig. 2*C*). Secondary shoots

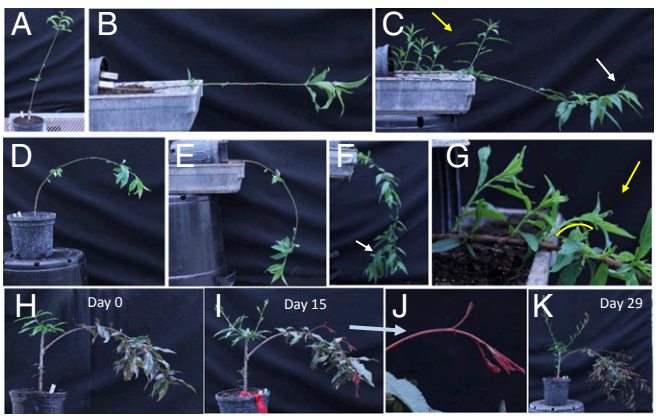

Fig. 2. Weeping peach trees did not respond to gravistimulation and were not rescued by GA treatment. (*A* and *B*) Standard tree before (*A*) and immediately after (*B*) 90° displacement. (*C*) Standard tree 20 d after displacement. (*D* and *E*) Weeping tree before (*D*) and after (*E*) 90° displacement. (*F* and *G*) Weeping tree 20 d after displacement. White arrows indicate shoot tip orientation. Yellow arrows indicate shoots that emerged after rotation. Yellow arc indicates the shape of new shoots. (*H*) Red-leafed weeping shoot grafted to standard green-leafed rootstock. (*I*) Grafted tree 15 d after GA treatment. (*J*) Close-up of a new weeping shoot 15 d after GA treatment. (*K*) Grafted tree 29 d after GA treatment.

PLANT BIOLOGY

Downloaded at Palestinian Territory, occupied on December 9, 2021

www.manaraa.com

that emerged from previously dormant buds on gravistimulated standard trees also exhibited upward bending and growth (Fig. 2*C*). In contrast, the shoot tips of weeping trees did not respond to the displacement. Their stems remained largely fixed in place and did not bend upward or downward. However, all new growth on reoriented weeping trees grew in a downward arcing fashion (Fig. 2 *D*–*G* and Fig. S1*A*). The downward growth ensued whether the primary shoot was repositioned to have an upward or downward orientation, revealing that bud positioning from development does not impact growth orientation (Fig. 2 and Fig. S1*A*). Additionally, displacing weeping trees by 90° so that their primary shoot was horizontal and perpendicular to the gravity vector did not result in any upward movement or growth (Fig. S1*B*). The mean branch tip angles of standard trees after rotation to horizontal was 54.7 (SD = 11.7) and for weep trees was −60.3 (SD = 3.0). It was unclear whether the downward angle in weep trees was entirely due to new growth or potentially the result of gravity acting on shoot tips that otherwise did not exhibit an upward bending response. Lastly, in response to the change in apical dominance from whole-tree reorientations, secondary shoots emerging from previously dormant buds on weeping trees arced downward after just a few centimeters of growth and continued growth in the direction of the gravity vector (Fig. 2*G* and Fig. S1*A*).

Branch growth and orientation is influenced by both local and systemic hormone signals. To investigate if there is an association between the weeping phenotype and systemic signals, buds from weeping peach trees were grafted onto standard peach rootstock and grown in the greenhouse for several seasons (Fig. 2*H*). On these trees, shoots from the standard rootstocks were also allowed to grow out above and below the graft. Grafted weeping buds emerged with the same weeping growth phenotype observed in ungrafted trees, suggesting that the weeping growth cannot be rescued by a mobile signal (Fig. 2*H*). Conversely, shoots from the standard rootstock above the graft exhibited a normal upright architecture (Fig. 2*H*). Collectively, these data suggest that WEEP encodes an autonomous determinant of shoot orientation for each branch.

Previously, it was reported that GA application could rescue the weeping trait and reverse the direction of growth in both peach and weeping cherry cultivars (24–26, 35). Likewise, in poplar, GA application was able to partially complement a poplar gravibending mutant line (3). To test whether our weeping germplasm responded similarly, GA was applied to greenhouse-grown weeping and standard trees derived from a segregating population and to standard trees with weeping shoots grafted onto them (Fig. 2 *H*–*K* and Fig. S1*C*). In both standard and weeping trees, GA treatment promoted the release of vegetative buds from dormancy, followed by rapid shoot growth. However, all new growth in the weeping shoots exhibited the characteristic downward growth, while the standard shoots had an upward orientation and growth trajectory (Fig. 2 *I*–*K* and Fig. S1*C*). Thus, the peach weeping phenotype described here could not be rescued by GA application.

Since the GA treatment experiment did not promote upright growth, we next investigated if there were differences in other endogenous phytohormones. Asymmetrical concentrations of auxin have long been associated with gravitropic bending responses (35). In addition, abscisic acid (ABA) has been shown to have an opposite role of auxin in gravitropism (36). Thus, concentrations of auxin (IAA) and ABA were measured in actively growing shoot tissues from four weeping and four standard 1-y-old greenhouse-grown trees. No significant differences between standard and weeping peach trees were found for either hormone (Fig. S1*D*). These results are consistent with the grafting experiment that weep phenotype is unlikely mediated by a defective mobile molecule such as a phytohormone.

Mapping of the Peach Weeping Locus and Identification of the Causative Allele. To identify the causative allele for peach weeping, a described whole-genome sequencing method (p-nome) was used (2, 7). DNA from 55 standard trees and 19 weeping trees was isolated from a segregating population and pooled by phenotype. The resulting pools were sequenced by using Illumina HiSeq technology to a coverage depth of 7× per weeping tree for the weeping pool and 2.5× per tree for the standard pool. The sequences from each pool were assembled to the peach genome (Version 1.0), and variants including single nucleotide polymorphisms (SNPs) and insertions or deletions (IN/DELs) that existed between the published genome and the pools were identified (37). A total of 644,488 variants were detected in the standard pool and 615,035 variants in the weeping pool (Datasets S1 and S2). The weeping variant list was then manually filtered against the standard pool for potential linkage (as described in *Methods*), and the remaining 4,659 variants were graphed by frequency over chromosomal position (Fig. 3*A* and Dataset S2). A total of 3,896 variants (84% of all variants) mapped to chromosome 3 (chr3) and produced a bell curve indicating the region of linkage (Fig. 3*A*). The peak of the curve spanned a 2-Mbp chromosomal region (between ∼14.2 and ∼16.2 Mbp) and contained 256 predicted genes (Fig. 3*A* and Dataset S2).

In an attempt to identify candidate genes within the locus, RNA sequencing (RNAseq) was performed by using shoot tips from a selected standard and weeping tree used in the mapping population, and differentially expressed genes (DEGs) located within the mapped region were identified (Dataset S3). *Ppa013325*, a gene located within the center of this region (on the minus strand between position 15,603,515 and 15,601,388) was expressed 127-fold less in the weeping tree compared with the standard (Dataset S3). No other gene in this region had an expression change of such a high magnitude. Inspection of the RNAseq assembly revealed that the small number of reads derived from the weeping pool spanned only the 3′ region of the gene (Fig. 3*B*). Subsequent examination of the genomic sequence alignments from both the weeping and standard p-nome pools revealed that the weeping alignment contained numerous broken paired-end reads and very minimal coverage, denoting a ∼1,374-bp deletion spanning part of the promoter and the 5′ end of gene *Ppa013325* (Fig. 3 *C* and *D* and Fig. S2). *Ppa013325*, also known as *Prupe.3G200700* in the peach genome version 2 (V2.0.a1; https://www.rosaceae.org/) is a single copy gene in peach (Fig. S2*D*).

To further investigate if this allele was associated with the weeping phenotype, fine mapping was performed by using 453 peach trees originating from four peach populations (three discrete lineages) that segregated for weeping (*Peach Weeping Plant Materials*). First, 125 trees located at the Appalachian Fruit Research Station, Kearneysville, WV, were tested, including 71 individuals from the p-nome population, 42 weeping trees from a related F2 population, and 12 trees from a segregating population with a different weeping lineage. SNP markers flanking *Ppa013325* at various intervals confirmed the locus and reduced the interval to a 502-Kb region (positions 15,537,956 and 16,040,400) (Dataset S4). Next, 328 trees comprising a segregating population at Institut National de la Recherche Agronomique (INRA) Unité de Génétique et Amélioration des Fruits et Légumes (UGAFL), France, were used for further fine mapping. First, a SNP linkage map using 91 segregating individuals was created by using a 9K peach SNP array (38). These results confirmed the position of the weeping locus (*pl*) to chr3 between position 15,203,630 and 16,351,739 (Fig. 3*E* and Dataset S4). Next, a series of flanking Kompetitive Allele-Specific PCR (KASP) markers were developed and tested on 237 additional weeping trees from the same population (Dataset S4). Based on identified recombinants, the locus was reduced to a ∼435-kb physical distance between 15,545,036 and 15,979,629 bp (Dataset S4). A KASP marker (AKSPP849) designed to detect the deletion in *Ppa013325* confirmed it to be homozygous in all weeping individuals and absent or heterozygous in all non-weeping individuals (Dataset S4).

Downloaded at Palestinian Territory, occupied on December 9, 2021
www.manaraa.com

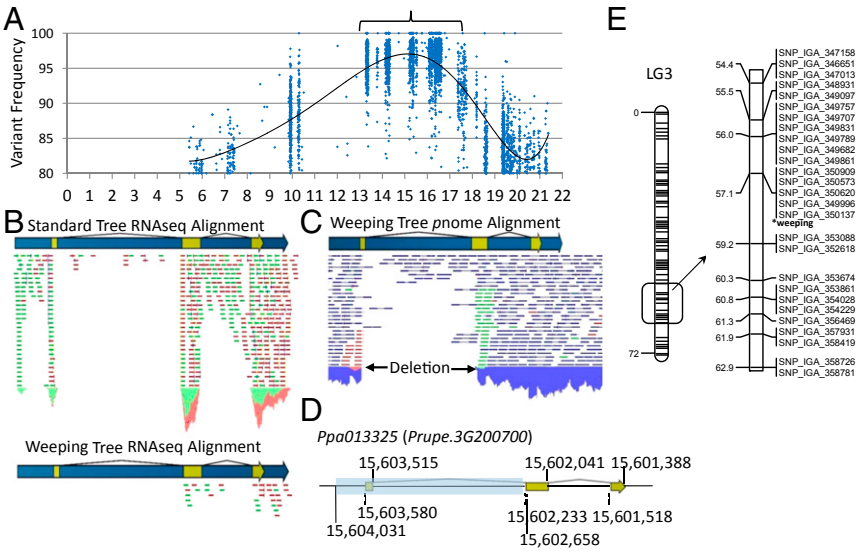

Fig. 3. Identification of a 5′ deletion of peach gene candidate *Ppa013325*. (*A*) *p*-nome map of DNA variants and corresponding map position in Megabase pairs on chr3. Dots represent single variants. Mapping interval defined by the curve peak is bracketed. (*B*) Alignment of RNA-sequencing reads from standard (*Upper*) and weeping (*Lower*) trees. Blue arrows represent *Ppa013325*. Yellow represents exons. Red and green lines signify aligned 50-bp sequencing reads. (*C*) Alignment of 100-bp paired-end weeping pool genomic sequence reads (blue) and broken paired reads (red and green) to *Ppa013325*. (*D*) Diagram of the wild-type *Ppa013325* gene and the mutant allele with the 5′ deletion (shaded region). Numbers indicate base pair positions. (*E*) Chr3 linkage map based on WP^2 population from 9K SNP mapping array.

Weeping peach traits are believed to have come from Chinese ornamental varieties that were integrated into European and US germplasm (39). KASP marker AKSPP849 was used to screen three Chinese weeping ornamental accessions that represent the diversity of weeping germplasm ("Hong Yu Chui Zhi," "Zhu Fen Chui Zhi," and "Yuan Yang Chui Zhi"). All three were homozygous for the deletion in *Ppa013325*. These results confirm the tight association between weeping and *Ppa013325* and suggest that the weeping trait studied here is of Chinese origin.

To rule out the possibility that a separate, tightly linked polymorphism could account for the weeping phenotype, the entire ∼435-kb locus was further analyzed. A total of 56 predicted genes were annotated within the locus, including *Ppa013325*. A total of 10 sequence variants were present in addition to the *Ppa013325* deletion. Eight were SNPs found in intergenic regions. The other two variants were single base IN/DELs (+T and −A, respectively) within homopolymeric intron sequences of *Ppa007938* and *Ppa006798*. Given that neither of these genes were differentially expressed in the RNAseq data and showed no differences in coding or splicing, they were deemed unlikely candidates for the *pl* allele. Based on the combined mapping data and lack of alternative gene variants within the mapped region, *Ppa013325* (*Prupe.*3G200700) was designated as the only candidate for WEEP (Fig. S2).

Silencing of the Plum WEEP Homolog Led to Nonvertical Shoot Growth and Branch Arcing. To confirm WEEP function, the expression of the homolog of *Ppa013325* was knocked down in plum (*P. domestica*) by RNAi-mediated silencing using the entire 390 bp peach WEEP CDS sequence. Since peach is not easily amenable to transformation, plum, a closely related species, can serve as a surrogate to study the function of peach genes (2, 40, 41). The potential for off-target gene silencing by the RNAi construct was determined to be minimal as the closest homologous WEEP sequence in the peach genome is only 18 nucleotides long (Fig. S2 *D* and *E*) (42).

Phenotypes of a total of 87 transgenic plums from 12 unique RNAi lines were visually assessed. Arcing phenotypes in primary shoots were visible in some plants when they reached ∼10–15 cm tall. Trees in 10 of 12 lines had nonvertical outward, curved, and/or wandering shoot orientations compared with transgenic empty vector control trees (Fig. 4 *A* and *B* and Fig. S3*A*). These wandering and outward phenotypes became more pronounced by the end of their second growing season (Fig. 4*C* and Fig. S3*A*).

WEEP expression analysis was performed by quantitative PCR (qPCR) on RNA from actively growing shoot tips (including meristem and young leaves) from plants in lines with six or more trees (nine lines total). Tissues were taken at the start of the second growing season when nonvertical growth was apparent. Only line 5, whose plants were phenotypically normal, did not show a significant decrease in WEEP expression compared with control plums (Fig. 4). Line 7 trees did not exhibit an abnormal shoot phenotype, although plants in this line had reduced levels of WEEP as measured by qPCR (Fig. S3 *A* and *B*). Such occasional discrepancies have been observed in plum RNAi lines (2, 41). Nonetheless, all trees from 10 of 12 lines (64 of 87 trees in total) exhibited nonvertical shoot growth and orientations.

The shoot phenotypes of representative lines (1, 5, and 10) exhibiting mild to severe phenotypes were chosen for quantitative analyses. Branches from each line along with plum controls were analyzed by fitting linear and elliptical models to the 2D representations of branches from these trees (Fig. S3*C*). The 2D representations were generated from motion tracker data (see *Methods* for details). In addition, standard and weeping peach tree branches were also analyzed (Fig. S3*B*). As expected, the individual standard peach and standard plum (cv. Stanley) branches fit linear models, while weeping peach branches fit elliptical models (Fig. 5 *A*–*C* and Fig. S3). The branch trajectories of RNAi plum lines fell in between the elliptical and linear models (Fig. 5 *D*–*F*). They had regions of curvature and linearity, exhibiting an intermediate phenotype (Fig. 5 *D*–*F*). Mean branch trajectories relative to vertical were calculated and were found to be wider than controls (Fig. S3*D*). The inability of WEEP silencing in plum to completely phenocopy peach weeping could be due to either residual levels of WEEP in the RNAi plums and/or background genetic differences between peach and plum.

WEEP Is an Ancient and Highly Conserved Gene with a Sterile Alpha Motif Domain. WEEP was found to be a highly conserved gene encoding a sterile alpha motif (SAM) domain protein that is typically present in other species as a single copy gene, except in plants that have undergone known whole-genome duplications (Fig. 6 and Figs. S2 *D* and *E* and S4). WEEP homologs were not found in the moss genome *Physcomitrella patens* or Chlorophyte genomes, but were present in the moss *Sphagnum phallax* and the genome of the lycophyte *Selaginella moellendorffii*. Phylogenetic analyses revealed known plant species relationships among angiosperms with the exception of the brassicaceae family, which contained five conserved amino acid changes and formed an out-group from other eudicots (Fig. 6 and Fig. S4). Four of these substitutions were located within the SAM domain (Fig. S4).

Downloaded at Palestinian Territory, occupied on December 9, 2021

www.manaraa.com

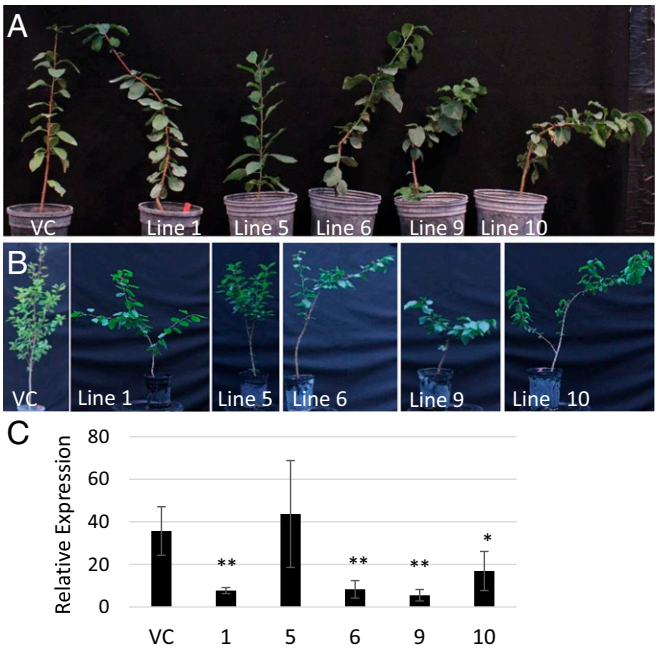

Fig. 4. RNAi-mediated silencing of WEEP led to nonvertical plum shoot orientations. (*A* and *B*) Representative WEEP RNAi plum trees after the first (*A*) and second (*B*) growing seasons. (*C*) Relative WEEP expression levels for corresponding plum lines. Bars represent SDs. VC indicates empty vector controls. Significance values are from Student's *t* test. $*P < 0.05$; $**P < 0.01$.

WEEP is known to be a single-copy gene in *Arabidopsis*. Kee et al. (43) reported that the *Arabidopsis* mutant (SALK153261) containing a T-DNA insertion within the WEEP ortholog *At3g07760* did not display a phenotype in rosettes or inflorescences. However, they also detected expression of the full-length gene in the mutant, suggesting the potential for residual expression (43). To definitively test that the loss of *At3g07760* does not lead to a weeping phenotype, the CRISPR-Cas9 system was used to create frame shift mutations in *At3g07760* in both the Landsberg erecta (*Ler*) and the Columbia (*Col-0*) backgrounds (Fig. 7 and Fig. S4). The two ecotypes were chosen because they have slightly different shoot architectures (*Ler* plants are shorter and stouter that *Col-0*). Using two different vectors, one targeting exon 1 and another targeting exon 2, 37 independent antibiotic-selected T1 CRISPR lines were generated and sequenced. Four were homozygous in the T1 generation. *weep-1* (line W4; c.948_949insA) and *weep-2* (line W5; c.948delA) were in the *Ler* background, while *weep-3* (line W11; c.G-14 > T & c.-8_-3insCTCTTC & c.-1_1insATC & c.1A > C) and *weep-4* (line W23; 948_949insA) were in the *Col-0* background. In agreement with Kee et al. (43), abnormal shoot phenotypes were not observed in multiple homozygous frame-shift mutant lines in either accession (Fig. 7).

WEEP Is Predominantly Expressed in Vascular Tissue. The relative expression of WEEP in vegetative peach tissues was assessed by qPCR. WEEP expression was highest in shoot tissues, particularly in tissues from whole-stem internodes and nodes, and it was absent in dormant vegetative buds (Fig. 8*A*). A further analysis of WEEP expression within stems was subsequently performed. RNA was extracted from hand-dissected xylem, phloem, and epidermal tissues from actively growing shoots. WEEP was predominantly expressed in phloem samples and to a lesser extent in xylem (Fig. 8*B*). WEEP expression was undetectable in epidermal tissues (Fig. 8*B*).

Transcriptomic Analyses of WEEP Trees. To identify possible regulatory roles of WEEP, an RNAseq study was performed by using total RNA extracted from sibling weeping and standard peach shoot tips collected from field-grown trees (Fig. 9, Fig. S5, and Dataset S5). A total of 1,294 genes were identified as DEGs between the two genotypes. MapMan was initially used to categorize the DEGs (Dataset S5) (44). Enriched gene categories including "amino acid metabolism," "cell," "cell wall," "DNA," "glycolysis," "metabolism," and "TCA cycle" were predominantly up-regulated in weeping peaches, while "photosynthesis" and "stress" genes were primarily down-regulated (Dataset S5). The numbers of up- and down-regulated DEGs in other enriched categories were approximately equal (Fig. S5 and Dataset S5). All DEGs were manually categorized to provide improved pathway resolution (Dataset S4).

In the manually curated categories, nearly all DEGs associated with "phloem" and "photosynthesis" were down-regulated while those in the "cell division/expansion," "cytoskeleton," "vesicle trafficking," "cell wall," and "auxin" categories were up-regulated (Fig. 9). The majority of the DEGs associated with auxin responses have known roles in mediating cell expansion, including auxin signaling repressors IAA7, IAA8, IAA9, IAA14, IAA16, IAA19, and ARF8 and 17 auxin-responsive Small Auxin Up RNA (SAUR)-like genes, as well as a set of genes known to modulate H (+) transport (Fig. 9 and Dataset S5). Notably absent were genes associated with auxin biosynthesis or perception. Coordinated changes were also observed with regard to other hormone responses, including GA (up-regulated), brassinosteroids (BR) (up-regulated), and ethylene (down-regulated), although the numbers of genes in these categories was relatively low (Fig. 9).

Discussion

Here, we identified a gene in trees required for directing branch orientation, possibly through altered gravity responses. The recessive mutant allele, a deletion in gene *Ppa013325* (aka *Prupe.3G200700*), was found to be present in diverse peach weeping germplasm in the United States, Europe, and China. WEEP encodes a 129-amino acid protein, of which more than half represents a domain in the SAM superfamily. SAM domain proteins are found throughout the plant and animal kingdoms, as well as in some bacteria, and have a wide range of functions (45). They include kinase signaling proteins, scaffolding proteins, RNA-binding proteins, and transcriptional activators or repressors (45). The SAM domain itself consists of bundles of alpha helices and is primarily known as a protein dimerization domain. However, there are also a few proteins for which the SAM

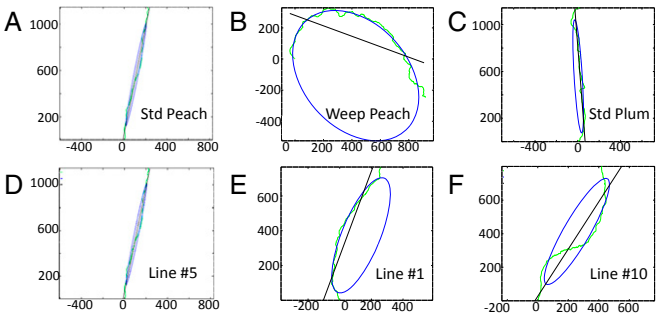

Fig. 5. Fit of peach and plum branch shapes to elliptical and linear models. Shown are the 2D representations of branches for standard peach (*A*), weeping peach (*B*), standard plum (*C*), and representative transgenic RNAi plum lines with no phenotype no. 5 (*D*), moderate phenotype no. 1 (*E*), and more severe phenotype no. 10 (*F*). Branch models (green) are transposed over best-fit elliptical (blue) and linear (black) models. The (0,0) position represents the base of a branch.

Downloaded at Palestinian Territory, occupied on December 9, 2021
www.manaraa.com

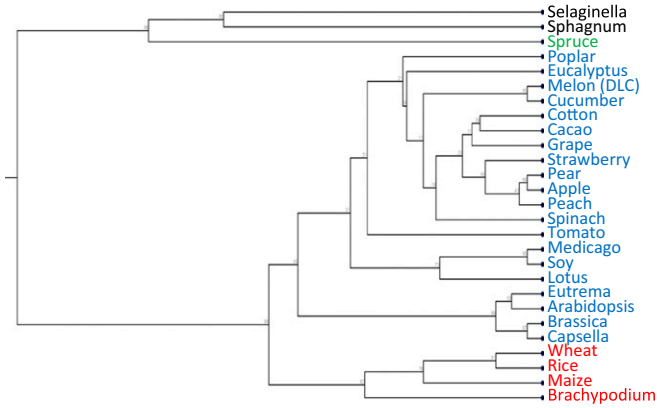

Fig. 6. Maximum-likelihood phylogenetic tree. Ancestral species are in black, gymnosperms are in green, monocots are in red, and eudicots are in blue. Protein IDs are in the legend for Fig. S3.

domain is an essential DNA- or RNA-binding domain (45–47). In plants, SAM domain proteins are poorly studied. Only 2 of the 13 *Arabidopsis* genes encoding putative SAM domains have been described to date. Although they share very limited similarity with WEEP, HYPOTHETICAL PROTEIN 30 (*HP30*) and *HP30-2* both are members of the preprotein and amino acid transporter family and code for translocase subunits involved in protein transport in chloroplasts and mitochondria (48, 49). While there is too little information to speculate a specific cellular mechanism for the WEEP protein at this time, the SAM domain of WEEP was found to be most similar to those that form self-assembling polymers and function as scaffolding proteins (50).

Phylogenetic analyses showed that WEEP was typically present as a single highly conserved gene in all vascular plants for which genome sequence was available. The absence of WEEP in *Physcomitrella* and algal genomes and presence in *Sphagnum* moss suggest that WEEP emerged during the evolution of plant vascular systems. Given the high level of amino acid identity, it is possible that WEEP function is conserved throughout diverse plant genera. Surprisingly, WEEP orthologs in *brassicaceae* formed a distinct clade separate from other eudicots due to five amino acid changes that were not found in other plant species. *Arabidopsis weep* mutants created via CRISPR did not display any measurable inflorescence shoot branching phenotypes, suggesting that WEEP function may have diversified in *brassica* species. Kee et al. (43) reported a WEEP homolog in melon (*Cucumis melo* L cv. Reticulatus), named Downward Leaf Curling (*CmDLC*). When *CmDLC* was overexpressed in *Arabidopsis*, the resulting plants produced downward-curling epinastic leaves. The leaf curling in these plants was associated with a reduction in abaxial epidermal cell size and number (43). This ectopic phenotype may imply a potential role for WEEP in modulating cell expansion and/or division. The function of the *Arabidopsis WEEP* gene, however, still remains enigmatic.

The downward elliptical branch growth characteristic of weeping peach trees was found to be relatively uniform. Evidence suggests this growth pattern is developmentally regulated, as the primary shoots of weeping peach seedlings, as well as mature tree shoots, have curved shoot tips, yet the shoots can grow vertically for a period of time before fully reorienting their growth downward. The silencing of WEEP in plum trees via RNAi suppression led to aberrant outward, nonvertical shoot growth, but the phenotype was less consistent. The branches of the WEEP RNAi-silenced trees more often had wandering orientations rather than a uniform curvature. This was presumably due to varying residual levels of WEEP expression in the plum RNAi lines, as indicated by qPCR measurements, and/or possible genetic differences between peach and plum. Also, at this time we cannot rule out the possibility of a second gene present in the *WEEP* locus that also contributes to the peach phenotype.

Using classical rotation experiments, we showed that weeping peach trees display a loss of the characteristic gravitropism responses of upward orientation and growth. Gravity sensing in plant shoots is known to occur in the endodermis, where the cells contain starch-filled amyloplasts that function as statoliths (36, 51–55). Upon sensing reorientation via changes in statolith sedimentation or positioning, an auxin polarization event driven by realignment of PIN auxin efflux carriers triggers the classic Cholodny–Went growth response, whereby cell elongation occurs along the bottom side of the stem to push shoot tips vertically (36, 56). The endodermis in trees, which is adjacent to the phloem, is present only in young shoot tissues, sloughing off as branches develop secondary growth. However, tree shoots can also sense gravity through specialized statolith-containing phloem cells (3, 57). Numerous studies in *Arabidopsis* have shown that plants lacking gravity sensing endodermal tissue, including shortroot (*shr*)/shoot gravitropism 1 (*sgr1*) and scarecrow (*scr*)/shoot gravitropism 7 (*sgr7*) mutants, have impaired shoot gravitropism (53, 54). Peach WEEP was highly expressed in the gravity-sensing tissues in trees. This localization pattern could support a possible role for WEEP in gravity-sensing or gravi-response.

In woody plants, which have stems that are rigid and cannot readily bend, gravitropic reorientation is also mediated via differential formation of reaction wood. In angiosperms, reaction wood manifests as the formation of specialized tension wood fibers that form on the upper side of stems to create a contractile force, essentially pulling stems upward (3, 57). Thus, gravitropic responses in trees are controlled by potentially two distinct processes: tip bending driven by cell expansion on the bottom side of the stem and reaction wood formation on the upper side of the stem. The weeping peach phenotype could be explained by a loss of tip gravitropism and/or an apparent reversal of reaction wood responses. Future investigations into the anatomy and chemical composition of the weeping branches are needed to evaluate these possibilities. In conjunction, mechanical strength tests are needed to fully evaluate if wood abnormalities in weeping peaches contribute to the weeping phenotype. Lastly, the possibility that neutral or negative phototropism contributes to the weeping phenotype should also be investigated.

GA was previously shown to potentiate reaction wood formation in trees by enhancing auxin transport across the stem via reorientation of the lateral auxin transporter PIN3 (3, 57). In poplar, GA application was able to partially compensate for a loss of reaction wood response in a gravibending mutant line (created by silencing *ARK3*) that did not form reaction wood (3). Likewise, GA application was reported to rescue weeping peach and cherry phenotypes via increased tension wood (24–26). Reches et al. (28) found that the lower half of actively growing

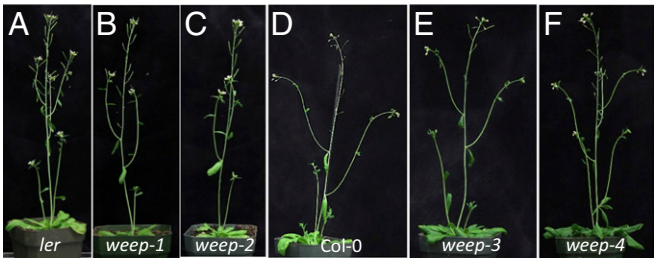

Fig. 7. *Arabidopsis weep* mutant lines in both ler and Col-0 backgrounds generated by CRISPR/Cas9 gene editing. (*A–C*) Ler control plant (*A*) and ler mutants *weep-1* (*B*) and *weep-2* (*C*). (*D–F*) Col-0 control plant (*D*) and Col-0 mutants *weep-3* (*E*) and *weep-4* (*F*).

PLANT BIOLOGY
Downloaded at Palestinian Territory, occupied on December 9, 2021
www.manaraa.com

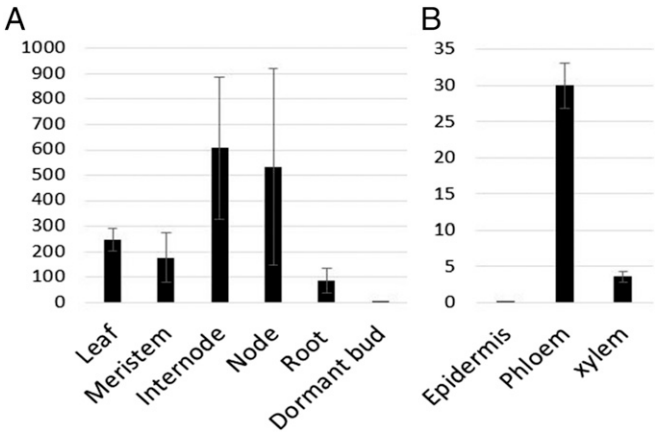

Fig. 8. Relative expression of WEEP in dissected tissues. Relative expression values were determined by qPCR. (*A*) WEEP expression in vegetative tissues from standard peach trees. (*B*) WEEP expression in dissected stems. Error bars represent SD.

weeping mulberry (*Morus alba Var. pendula*) tree branches had significantly greater GA levels than the upper side. Curiously, GA applications did not rescue our peach weeping phenotype. This lack of reversion was not due to GA insensitivity, as the GA treatment resulted in the release of dormant buds and rapid shoot elongation that are hallmarks of GA responses. These findings suggest that our weeping germplasm may have a different origin than the published weeping peach study. Our results could suggest that WEEP regulates branch orientation independent of the influence of GA on wood development. Alternatively, our concentration, application method, and timing of treatments may not have been optimal for inducing tension wood formation in our peach germplasm, despite its ability to promote active growth.

The previously described genetic interaction between the *tac1* and *weep* alleles in peach may also imply a role for WEEP in plant responses to gravity, as pillar (*tac1*) branches all grow vertically. While a specific function for *TAC1* is unknown, this gene is a member of the IGT gene family that includes the gravitropic regulator *LAZY1*, which acts upstream of polar auxin transport (10, 12–14). However, the constitutive elliptical growth phenotype in weeping peach is unique from other described plant gravitropic mutants.

Transcriptome analyses revealed a potential mechanistic connection to gravity response, as numerous genes associated with auxin, cell division, cell wall and cytoskeleton composition, and vesicle trafficking were coordinately up-regulated in weeping shoot tips. These gene categories are all known to be essential signaling components of gravitropic responses. Asymmetric cell divisions and/or expansion is critical for shoot and root bending, as are modifications of cytoskeleton composition (36). In the endodermis, vacuole membrane structures and proper vesicle trafficking are influenced by cytoskeleton composition, and both are essential for gravitropic responses in plant shoots (53, 55, 58–63). In addition, changes in expression of auxin-signaling genes, including *IAA-AUX* genes, *ARF8*, *PILS5*, and numerous *SAURs* could coincide with the altered gravitropic responses in weeping peach, despite the lack of measurable differences in auxin concentrations. Auxin has long been known as a key player in shoot growth orientation and reorientation in response to gravistimulation. Auxin is also involved in reaction wood development (3, 57, 64, 65). Intriguingly, overexpression of *PILS5* (which was increased in weeping shoots) was previously shown to lead to agravitropic growth in *Arabidopsis* seedlings via altered auxin response maximum and/or decreased cellular retention of auxin (66).

Genes associated with cellular and apoplastic acidification were also strongly differentially expressed in weeping peach shoots. Current evidence suggests that, in response to auxin, SAUR proteins inhibit PP2C phosphatases to activate (H^+) ATPase pumps via dephosphorylation, resulting in acid-mediated cell well expansion. Seventeen SAURS were more highly expressed in weeping peach shoot tips (67). The auxin-responsive gene AVP1 H^+ ATPase, which functions in both vacuolar and apoplastic acidification, was also up-regulated along with three vacuolar H^+ ATPases (68). Likewise, genes with similarity to peptide growth hormone receptors (PSKR and PSYR) and PSK peptide precursor were substantially down-regulated (69). Combined, these signaling pathways function to control cell expansion via direct modulation of plasma membrane H^+ ATPase activity and apoplastic acidification (70). Lastly, three auxin responsive cytochrome b561 electron transport proteins were induced in weeping peach shoots, which are thought to stimulate H^+ ATPase pumps via plasma membrane depolarization (71).

In summary, we have found that WEEP, a highly evolutionarily conserved SAM domain protein, is a key factor in regulating branch orientation in peach trees. WEEP appears to act autonomously and/or downstream of gravitropic hormone signaling pathways. The predominant expression of WEEP in endodermal tissues indicates that WEEP acts in cells normally associated with gravity sensing and gravi-bending growth. While much more experimentation is needed to investigate its molecular function, the identification of this gene from weeping peach lays the foundation for determining mechanisms of branch orientation and gravitropic responses in woody trees.

Methods

The 3D Tree Reconstruction and Shape Analyses. A representative WEEP tree was analyzed by using an in-house-designed structural phenotyping system at the US Department of Agriculture, Agricultural Research Service Appalachian Fruit Research Station, Kearneysville, WV (72–75). Briefly, the tree was imaged against a blue background via a robotic arm with two digital cameras

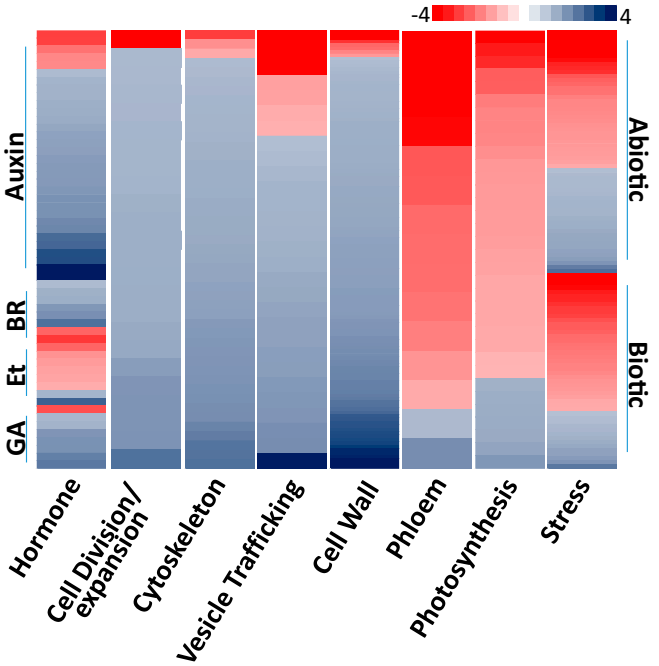

Fig. 9. Global differences in gene expression determined by RNAseq analyses. Heat map showing coordinated expression patterns among various enriched gene categories. Scale bar is shown at top. Subcategories of genes in "hormone" and "stress" categories are shown to the side.

Downloaded at Palestinian Territory, occupied on December 9, 2021
www.manaraa.com

mounted on the robot's end effector. A total of 63 images were acquired from various positions around the tree, and algorithms were used to dissect tree vs. nontree pixels in each image. The reconstruction step utilized a separate algorithm that calculated the 3D shape most likely to have produced the images of the tree (72, 73). The tree's branching structure was extracted from the reconstruction through a curve skeletonization algorithm, and other attributes, such as branch radius, branch angle, and branch length, were computed from the branching structure and reconstruction.

An ellipse is a 2D shape that can be represented in standard form by using two parameters representing the major (*a*) and minor (*b*) axis:

$$\frac{x^2}{a^2}+\frac{y^2}{b}=1. \quad [1]$$

A program was written to find the best-fit ellipse parameters for each selected branch. Since the branches are 3D, they were first transformed to two dimensions by finding the best-fit plane and projecting the branch points to that plane. The general equation for conic sections is:

$$Ax^2+Bxy+Cy^2+Dx+Ey+F=0. \quad [2]$$

The parameters of the conic section were determined by fitting the projected branch points to this equation. From [**2**], the elliptical standard form parameters were extracted including the major (*a*) and minor (*b*) axis. In addition, minimum and maximum curvature was computed for each ellipse.

Quantitative Analysis of Branch Shape Using Motion Tracker Data. The motion tracker data were generated by using a G4 motion tracker (Polhemus). The electromagnetic source was positioned at the base of each tree. The *z* axis of the electromagnetic source was aligned to gravity. To record branch shape, the sensor was moved by hand along each branch, tracing the shoots. Multiple branches from three to six trees of each type of tree were traced. Positional data were smoothed to remove abrupt movements caused by axillary shoots and leaf petioles. The data were then constrained to a plane orthogonal to the *x*–*y* plane. The ellipse fitting was performed on the 2D representations by using the method of Halir and Flusser (76), and the line fitting was performed by using standard least squares. The elliptical features such as the length of the major and minor axes and the angle of rotation were computed from the best-fit ellipse parameters. The branch angle relative to the vertical was computed from the vector formed from the elliptical semimajor axis; its units are degrees. This procedure was automated with software written in C++.

DNA Isolation. DNA for genomic sequencing and genotyping was extracted by using the Omega Bio-Tek EZNA SQ Plant DNA extraction kit with the RNase step (catalog no. D3095-01). DNA concentrations for sequencing were calculated by using the Molecular Probes QuantiT PicoGreen dsDNA Assay (catalog no. P11496; Life Technologies). DNA isolation at UGAFL was performed by using the DNeasy 96 Plant kit (Qiagen).

Genomic Sequencing and P-Nome Mapping. DNA from 19 weeping and 55 standard trees from the Kv050168 population was pooled by phenotype. DNA from each tree was quantified and diluted appropriately to ensure equal representation of individuals in the pool. The DNA pools, with final concentrations between 2.5 and 4 μg, were sent to the genomics resources core facility at Weill Cornell Medical College (New York) and 100-bp paired-end sequencing was performed by using an Illumina HiSeq 2000. A total of 355,011,274 raw reads were generated for the weep pool and 367,203,548 for the standard pool. Raw reads were imported into CLC Genomics workbench (Version 6.1) and trimmed on quality (with an ambiguity limit of two nucleotides and a quality limit of 0.05). Reads <75 nucleotides in length were removed. The remaining 354,634,975 weeping and 366,694,736 standard reads were aligned to the peach genome (Version 1.0 scaffolds) (37). Next, the probabilistic variant detection function in CLC was performed on both alignments with the following settings: Ignore nonspecific matches; ignore broken pairs; minimum coverage 25; variant probability 90; requires presence in both forward and reverse reads; maximum expected variants 2. The weeping pool sequencing reads contained 1,156,590 variants, while the standard pool contained 1,221,826. Variant data were then exported into Excel for manual filtering. All variants in the weeping pool with a frequency <80% were removed, as were variants in the weeping pool with a forward/reverse balance <10%, and variants with coverage >500 were removed. Next, the variants present in the standard pool with frequencies >45% and <20% were removed from the weeping variant list.

RNA Extraction, Sequencing, and Transcriptome Analysis. Total RNA was isolated from ∼3–6 cm of actively growing shoot tips (with leaves removed) from one weeping and one standard peach tree from the mapping population. RNA was extracted by using the Omega SQ Total RNA kit with 2% polyvinylpyrrolidone added to the red cell lysis buffer, followed by a DNase step using Ambion Turbo DNA free. Approximately 3 μg of RNA was sent to the genomics resources core facility at Weill Cornell Medical College, where RNA TruSeq 50-bp unpaired libraries were prepared for each and sequenced in the same lane by using an Illumina HiSeq 2000. Raw sequencing data were uploaded to the CLC Genomics Workbench and trimmed based on quality (setting at 0.05) and ambiguity (maximum 2 ambiguous nucleotides allowed). The remaining 86,592,113 reads from the weeping tree and 77,747,375 reads from the standard tree were aligned to the peach genome (Version 1.0) by using CLC Genomics Workbench with the following parameters: additional upstream and downstream bases = 500; max number of mismatches = 2; minimum length fraction = 0.9, minimum similarity fraction = 0.8; unspecific match limit = 10; No strand specific assembly; strand = forward; no exon discovery; minimum exon coverage fraction = 0.2; minimum number of reads = 10; expression value = RPKM. Differential expression was determined using the "Transcriptomics Analysis" functions in CLC.

For transcriptome studies, total RNA was isolated (using the method described above) from three ∼6- to 10-cm length shoot tips (with leaves removed) from each of four standard and four weeping 10-y-old field-grown peach trees from the Kv991636 population (described above). Approximately 4 μg of total RNA was sent to Cornell Weill Genomics for 50-bp single-pass sequencing. Raw reads were uploaded into CLC Bioinformatics Workbench, where they were trimmed as described above. Remaining reads were aligned to the peach genome by using CLC with the following settings: maximum number of hits for a read = 10; count paired reads as two = No; Expression value = RPKM; no global alignment; similarity fraction = 0.95; length fraction = 0.8; mismatch cost = 2; insertion cost = 3; deletion cost = 3. Expression analysis using these alignments was then performed by using the Transcriptomics Analysis function and normalized by totals with counts representing reads per 1,000,000. Statistical analysis was done by using Baggerley's test, and DEGs with a false discovery rate value ≤0.05 were used for further analysis. Data were exported to Excel, and corresponding *Arabidopsis* homologs of the peach genes were added. Weighted proportions fold changes were entered into MapMan (Version 3.5.1) to identify highly DEG categories using the *P. persica* phytozome v9 gene mapping. MapMan categories with significant enrichment ($P \leq 0.05$), based on the Benjamini–Hochberg-corrected Wilcoxon rank sum test, were identified. The DEG list was then further manually annotated to refine the categories, subcategories, and their associated genes.

WEEP Mapping and Genotyping. High-resolution melting (HRM) was performed by using MeltDoctor HRM Master Mix (Applied Biosystems), according to the manufacturer's protocol, and the reactions were run on a ViiATM Real-Time PCR System instrument (Applied Biosystems) as described (2). For standard PCR genotyping, the following primers were used to detect the weeping mutants: PpWEEP-Del-genotype-F2 5′ (GATTGTGAAGGACACGTAGCT) and PpWEEP-Del-genotype-R2 (5′ TGTCTGTAACTTGGCTGTGTTTA) using an annealing temperature of 63° to produce a ∼300-bp amplicon. Primers used to detect the wild-type allele were PpWEEP Del internal F2 (5′ TGTTGTTTGGGACATCTGAT) and PpWEEP Del internal R2 (5′ AGCAGATTACATGAAAAGTCTCCT) with an annealing temperature of 56° to produce a 279-bp amplicon.

Genotyping of the UGAFL peach populations [91 trees of the F2 peach population (known as the WP^2 population)] was performed by using the International Peach SNP Consortium 9K peach SNP array (Version 1; Illumina Inc.) (38). For SNP array genotyping, isolation of genomic DNA and subsequent Infinium II assays were performed as described in Verde et al. (38). DNA was diluted to a concentration of 50 ng/μL and sent to the Istituto Agrario San Michele all'Adige Research and Innovation Centre (San Michele all'Adige, Italy) for genotyping. The assays were performed by following the manufacturer's recommendations. SNP genotypes were scored with the Genotyping Module of GenomeStudio Data Analysis software (Illumina Inc.), by using a GenCall threshold of 0.15. SNPs with GenTrain scores <0.6 were used to clean up the data file. SNPs showing severe segregation distortion (χ^2 test, $P < 10^{-6}$) and >1% of missing data were excluded. Linkage mapping at UGAFL was processed as follows. For the WP^2 map, linkage analyzes were performed by using JoinMap (Version 4.1) (77). The recombination fraction value was set at 0.4, and the initial minimum logarithm of odds score threshold at 3. Recombination frequencies were converted into marker distances by using the Kosambi mapping function (78). The quality of markers was checked, and those with a high number of missing/conflicting (repetitions) data were discarded. In a second step, "non-useful" markers were discarded like those monomorphic in the population or those presenting a very high degree of segregation distortion (χ^2 test). Only

Downloaded at Palestinian Territory, occupied on December 9, 2021
PLANT BIOLOGY
www.manaraa.com

polymorphic SNPs homozygous in both parents (AA×BB) were used to construct the genetic map of WP[2]. Map was drawn by using MapChart software (79), and the order and distribution of markers on the genetic map were compared with their positions in the peach sequence (Version 1.0).

For fine mapping of the remaining WP[2] trees, KASP markers were designed at UGAFL-INRA based on SNPs from the peach 9K SNP array, the 40K SNP array, and the genomic sequence of peach *weep* (clone S2678). Primer sequences were sent to MWG-Biotech to synthesize the corresponding KASP markers. The reaction mixture for each marker was prepared according to the manufacturer protocol. After validation by using DNAs from S2678 and S6146 parents, fluorescent endpoint genotyping of 237 individuals was conducted by using the 2103 EnVision Multilabel Reader (Perkin-Elmer Co.). After completion of fine mapping *pl* to the region between KASP markers AKSPP378 and AKSPP780, the allele-specific KASP AKSPP849 marker was developed based on the sequence of S2678 and the location of the deletion detected in *Ppa013325*.

Protein Alignments and Phylogenetic Tree Construction. Protein alignments were generated by using Muscle (Version 3.8.425) (80). A maximum-likelihood phylogenetic tree was generated in CLC Genomics Workbench by using the UPGMA algorithm with Kimura distance measurements and 100 bootstrap replicates.

***Arabidopsis* WEEP CRISPR Lines.** CRISPR constructs were generated to target both the first and second exons in At3g07760. The target sequence for the first exon was AAGAAATCAAGAGGCTCGGG (located on the minus strand), while the exon of the second target sequence was AGATCCTTCACTTCATAAGG. To generate the CRISPR construct targeting the first exon of the *Arabidopsis* WEEP gene (AT3G07760), primers 5′-ATTGAAGAAATCAAGAGGCTCGGG-3′ and 5′-AAACCCCGAGCCTCTTGATTTCTT-3′ were used to generate the single guide RNA (sgRNA) insert fragment. The sequences provide overhangs that facilitate ligation of the sgRNA insert with BsaI digested pHEE401E vector, that contains an egg cell-specific promoter (81). CRISPR construct targeting the second exon of *Arabidopsis* WEEP gene was created in the same fashion by using primers 5′-ATTGAGATCCTTCACTTCATAAGG-3′ and 5′-AAACCCTTATGAAGTGAAGGATCT-3′. The resulting constructs were sequenced and transformed into *Agrobacterium tumefaciens* strain GV3101. *Arabidopsis* ecotypes *Ler* and Col-0 were transformed with *Agrobacterium* harboring the CRISPR construct by floral dipping (82). Transformed plants were selected on 1/2 Murashige and Skoog plates containing 30 μg/mL hygromycin. To identify plants with mutations, the appropriate exon region from T1 plants was amplified by either AtWEEP CRISP Ex 1 seq F (5′ GCATTTTGGCACAGTTAAGTT) and AtWEEP CRISP Ex 1 seq R (5′ ATTGGATCAAACAACAAGAACA) to amplify the first exon or AtWEEP CRISP Ex 2 seq F (5′ TTGTTCTATCAGATGCTATTATGGA) and AtWEEP CRISP Ex 2 seq R (TCAAGATTCAAGCTTGAGAGATAC) to amplify the second exon. Amplicons were then sequenced by using the forward primer. Homozygous mutant lines were selected for subsequent T2 analysis. After hygromycin selection, both T1 and T2 plants were transplanted to MetroMix 360 soil (SunGro) and grown in 4″ pots under 16-h light (~80 μM) in a controlled environment chamber set at 20° and 65% humidity.

Generation of the WEEP Silencing Vector and Transgenic Plums. The 396-bp peach WEEP CDS was amplified from RNA from a standard peach tree with the SuperScript III one-step RT-PCR kit with Platinum Taq (Invitrogen/Thermo Fisher Scientific) and primers PpWEEP-CDS-F-SAL1 (5′-ATGTCGACGGCGTTATGATGAGGGAGAT) and PpWEEP-CDS-R (STP)-SmaI (5′-ATCCCGGGTTATGGTTCCAGCTTCAAGGA). The amplicon was then cloned into the Invitrogen pCR8/GW/TOPO vector before being transferred into the hairpin silencing vector pHellsgate 8 through LR reaction. The WEEP pHellsgate 8 was subsequently transformed into *A. tumefaciens* GV3101. Seeds from the plum cultivar "Stanley" were transformed by using described hypocotyl slice tissue culture methods (41).

qPCR to Determine the Levels of WEEP Expression. The RNA extraction method was the same as described above for RNAseq with the exception that the RNA Clean and Concentrate kit (Zymo Research) was used for RNA purification instead of phenol:chloroform. WEEP expression levels were determined by qPCR using SuperScript III Platinum SYBR Green One-Step qRT-PCR Kit with Rox (Invitrogen/Thermo Fisher Scientific) and run on an ABI7900 (Applied Biosystems). 50 ng of total RNA were used for each reaction. Primers used for peach gene expression were Ppweep-qPCR-1F (5′ CGTGATTGTCTGTTACGCTTTGC) and Ppweep-qPCR-1R (5′ TCACGCTGTGTAAGGAACTAAGGC). The primers for amplifying native gene expression in plum were designed based on the alignment of plum sequences to the peach genome, as the assembly of the hexaploid *P. domesta* genome assembly is incomplete. The plum primer sequences were 5′ TGCCTAGAGAACAGAGTAGGAAAG (WEEP-qPCR-UTR-F) and 5′ GACCAGCGATAGATACATTAAAGGC (WEEP-qPCR-UTR-R). Primers for both peach and plum qPCR were designed to detect only WEEP expression and melt curve analyses confirmed primer specificity as only one amplicon was produced by the qPCR reactions. Relative expression values were determined from standard curves generated using known amounts of total RNA from standard plum and peach trees. For expression in the transgenic plums, three to six biological replicates sampled from clonal plants were tested, and each was run with three technical replicates. Expression in peach tissues was determined from between two and four biological replicates, each with three technical replicates.

GA Treatment. Two standard peach trees with weeping branches from prior bud grafts, three weeping trees, and three standard trees, all in 8″ pots, were sprayed twice a week for 1 mo with 1,000 ppm GA3 (0.01%) (in the form of ProGibb; Valent BioSciences Corp.) in the greenhouse. An additional three weeping and three standard trees were sprayed with water. All trees were removed from cold dormancy ~1 mo before treatments.

Hormone Analysis. Phytohormone analysis was performed by using four biological replicates each of weeping and standard trees (Proteomics & Mass Spectrometry Facility, Danforth Plant Science Center, St. Louis MS). A total of 200 mg of fresh tissues was harvested from young actively growing peach shoot tips sampled from four weeping and four nonweeping greenhouse grown trees.

ACKNOWLEDGMENTS. We thank Mark Demuth for generating and maintaining the Appalachian Fruit Research Station (AFRS) peach populations in the field and Doug Raines and Isiah Acly for assistance with plant care. Cheryl Vann assisted with statistical analyses. Peach gravitropism experiments were performed by Emma Acly. We thank Frank Telewski for insight into gravitropism and phototropism in preparation of this manuscript; Elodie Lecerf, Virginie Diévart, and Carole Confolent for their technical assistance and advice; the technical staff of the experimental team of the UGAFL for their help; Jehan-Baptiste Mauroux (FruitBreedomics at UGAFL) for assistance in fine mapping; and the MGX-Montpellier GenomiX facility for their assistance with sequencing and alignment of the peach variety Weeping Flower Peach cl. S2678. We are grateful for genome access and tools provided by the International Peach Genome Initiative and the Genome Database for Rosaceae. The work at AFRS was supported by US Department of Agriculture National Institute of Food and Agriculture Agriculture and Food Research Initiative Competitive Grant 10891264 and by National Science Foundation Grant 1339211. The work at UGAFL was partly funded by grants from the INRA Plant Biology and Breeding division through the InnovaFruit 1 project and under the European Union Seventh Framework Programme by the FruitBreedomics Project 265582. The Proteomics and Mass Spectrometry Facility that performed hormone quantification is supported by instrumentation funding from National Science Foundation Grant SBI-0521250 for acquisition of the QTRAP LC-MS/MS.

1. Wilson BF (2000) Apical control of branch growth and angle in woody plants. *Am J Bot* 87:601–607.
2. Hollender CA, Hadiarto T, Srinivasan C, Scorza R, Dardick C (2016) A brachytic dwarfism trait (dw) in peach trees is caused by a nonsense mutation within the gibberellic acid receptor PpeGID1c. *New Phytol* 210:227–239.
3. Gerttula S, et al. (2015) Transcriptional and hormonal regulation of gravitropism of woody stems in Populus. *Plant Cell* 27:2800–2813.
4. Wolters PJ, Schouten HJ, Velasco R, Si-Ammour A, Baldi P (2013) Evidence for regulation of columnar habit in apple by a putative 2OG-Fe(II) oxygenase. *New Phytol* 200:993–999.
5. Okada K, et al. (2016) Expression of a putative dioxygenase gene adjacent to an insertion mutation is involved in the short internodes of columnar apples (*Malus* × *domestica*). *J Plant Res* 129:1109–1126.
6. Otto D, Petersen R, Brauksiepe B, Braun P, Schmidt ER (2014) The columnar mutation ("Co gene") of apple (*Malus domestica*) is associated with an integration of a Gypsy-like retrotransposon. *Mol Breed* 33:863–880.
7. Dardick C, et al. (2013) PpeTAC1 promotes the horizontal growth of branches in peach trees and is a member of a functionally conserved gene family found in diverse plants species. *Plant J* 75:618–630.
8. Yu B, et al. (2007) TAC1, a major quantitative trait locus controlling tiller angle in rice. *Plant J* 52:891–898.
9. Ku L, et al. (2011) Cloning and characterization of a putative TAC1 ortholog associated with leaf angle in maize (*Zea mays* L.). *PLoS One* 6:e20621.
10. Hollender CA, Dardick C (2015) Molecular basis of angiosperm tree architecture. *New Phytol* 206:541–556.

Downloaded at Palestinian Territory, occupied on December 9, 2021
www.manaraa.com

11. Yoshihara T, Spalding EP, Iino M (2013) AtLAZY1 is a signaling component required for gravitropism of the *Arabidopsis thaliana* inflorescence. *Plant J* 74:267–279.
12. Yoshihara T, Iino M (2007) Identification of the gravitropism-related rice gene LAZY1 and elucidation of LAZY1-dependent and -independent gravity signaling pathways. *Plant Cell Physiol* 48:678–688.
13. Li P, et al. (2007) LAZY1 controls rice shoot gravitropism through regulating polar auxin transport. *Cell Res* 17:402–410.
14. Dong Z, et al. (2013) Maize LAZY1 mediates shoot gravitropism and inflorescence development through regulating auxin transport, auxin signaling, and light response. *Plant Physiol* 163:1306–1322.
15. Uga Y, et al. (2013) Control of root system architecture by DEEPER ROOTING 1 increases rice yield under drought conditions. *Nat Genet* 45:1097–1102.
16. Guseman JM, Webb K, Srinivasan C, Dardick C (2017) DRO1 influences root system architecture in *Arabidopsis* and *Prunus* species. *Plant J* 89:1093–1105.
17. Darwin C (1868) The variation of animals and plants under domestication. *Animals (Basel)* 1:1–411.
18. Sampson DR, Cameron DF (1965) Inheritance of branzage foliage, extra petals and pendulous habit in ornemental crabapples. *Proc Am Soc Hortic Sci* 86:717–722.
19. Brown SK, Maloney KE, Hemmat M, Aldwinckle HS (2004) Apple breeding at Cornell: Genetic studies of fruit quality, scab resistance and plant architecture. *Acta Horticulturae* 663:15–20.
20. Dougherty L, Singh R, Brown S, Dardick C, Xu K (2018) Exploring DNA variant segregation types in pooled genome sequencing enables effective mapping of weeping trait in Malus. *J Exp Bot* 69:1499–1516.
21. Roberts DJ, Werner DJ, Wadl PA, Trigiano RN (2015) Inheritance and allelism of morphological traits in eastern redbud (*Cercis canadensis* L.). *Hortic Res* 2:15049.
22. Kotobuki K, Sawamura Y, Saito T, Takada N (2005) The mode of inheritance of weeping habit in Japanese chestnut, *Castanea crenata*. *Acta Hortic* 693:477–484.
23. Zhang J, et al. (2015) High-density genetic map construction and identification of a locus controlling weeping trait in an ornamental woody plant (*Prunus mume* Sieb. et Zucc). *DNA Res* 22:183–191.
24. Baba K, et al. (1995) Induction of tension wood in GA3-treated branches of the weeping type of Japanese cherry, *Prunus spachiana*. *Plant Cell Physiol* 36:983–988.
25. Nakamura T, et al. (1994) The effects of GA3 on weeping of growing shoots of the Japanese cherry, *Prunus spachiana*. *Plant Cell Physiol* 35:523–527.
26. Nakamura T, Saotome M, Tanaka H (1995) Weeping habit and gibberellin in *Prunus*. *Acta Hortic* 394:273–280.
27. Sugano M, Nakagawa Y, Nyunoya H, Nakamura T (2004) Expression of gibberellin 3 beta-hydroxylase gene in a gravi-response mutant, weeping Japanese flowering cherry. *Biol Sci Space* 18:261–266.
28. Reches S, Leshem Y, Wurzburger J (1974) On hormones and weeping: Asymmetric hormone distribution and the pendulous growth habit of the weeping mulberry, *Morus alba* var. pendula. *New Phytol* 73:841–846.
29. Bassi D, Dima A, Scorza R (1994) Tree structure and pruning response of 6 peach growth forms. *J Am Soc Hortic Sci* 119:378–382.
30. Werner DJ, Chaparro JX (2005) Genetic interactions of pillar and weeping peach genotypes. *HortScience* 40:18–20.
31. Chaparro JX, Werner DJ, O'Malley D, Sederoff RR (1994) Targeted mapping and linkage analysis of morphological isozyme, and RAPD markers in peach. *Theor Appl Genet* 87:805–815.
32. Bassi D, Rizzo M (2000) Peach breeding for growth habit. *Acta Hortic* 538:411–414.
33. Monet R, Bastard Y, Gibault B (1988) Etude génétique du caractère port pleureur chez le pêcher. *Agronomie* 8:127–132.
34. Dirlewanger E, Bodo C (1994) Molecular genetic mapping of peach. *Euphytica* 77:101–103.
35. Yoshida M, Nakamura T, Yamamoto H, Okuyama T (1999) Negative gravitropism and growth stress in GA3-treated branches of *Prunus spachiana* Kitamura f. spachiana cv. Plenarosea. *J Wood Sci* 45:368–372.
36. Toyota M, Gilroy S (2013) Gravitropism and mechanical signaling in plants. *Am J Bot* 100:111–125.
37. Verde I, et al.; International Peach Genome Initiative (2013) The high-quality draft genome of peach (*Prunus persica*) identifies unique patterns of genetic diversity, domestication and genome evolution. *Nat Genet* 45:487–494.
38. Verde I, et al. (2012) Development and evaluation of a 9K SNP array for peach by internationally coordinated SNP detection and validation in breeding germplasm. *PLoS One* 7:e35668.
39. Hu D, Zhang Z (2005) Genetic relationship of ornamental peach determined using AFLP markers. *HortScience* 40:1782–1786.
40. Guseman JM, Webb K, Srinivasan C, Dardick C (2017) DRO1 influences root system architecture in *Arabidopsis* and *Prunus* species. *Plant J* 89:1093–1105.
41. Petri C, Webb K, Hily J-M, Dardick C, Scorza R (2008) High transformation efficiency in plum (*Prunus domestica* L.): A new tool for functional genomics studies in *Prunus* spp. *Mol Breed* 22:581–591.
42. Senthil-Kumar M, Mysore KS (2011) Caveat of RNAi in plants: The off-target effect. *RNAi and PLant Gene Function Analysis Methods and Protocols*, eds Kodama H, Komamine A (Springer, New York), pp 13–26.
43. Kee J-J, et al. (2009) Overexpression of the downward leaf curling (DLC) gene from melon changes leaf morphology by controlling cell size and shape in *Arabidopsis* leaves. *Mol Cells* 28:93–98.
44. Thimm O, et al. (2004) MAPMAN: A user-driven tool to display genomics data sets onto diagrams of metabolic pathways and other biological processes. *Plant J* 37:914–939.
45. Johnson DH (2006) The many faces of replication. *Crop Sci* 40:2486–2491.
46. Schultz J, Ponting CP, Hofmann K, Bork P (1997) SAM as a protein interaction domain involved in developmental regulation. *Protein Sci* 6:249–253.
47. Slaughter BD, Huff JM, Wiegraebe W, Schwartz JW, Li R (2008) SAM domain-based protein oligomerization observed by live-cell fluorescence fluctuation spectroscopy. *PLoS One* 3:e1931.
48. Rossig C, et al. (2013) Three proteins mediate import of transit sequence-less precursors into the inner envelope of chloroplasts in Arabidopsis thaliana. *Proc Natl Acad Sci USA* 110:19962–19967.
49. von Zychlinski A, et al. (2005) Proteome analysis of the rice etioplast: Metabolic and regulatory networks and novel protein functions. *Mol Cell Proteomics* 4:1072–1084.
50. Meruelo AD, Bowie JU (2009) Identifying polymer-forming SAM domains. *Proteins* 74:1–5.
51. Morita MT (2010) Directional gravity sensing in gravitropism. *Annu Rev Plant Biol* 61:705–720.
52. Fukaki H, et al. (1998) Genetic evidence that the endodermis is essential for shoot gravitropism in *Arabidopsis thaliana*. *Plant J* 14:425–430.
53. Hashiguchi Y, Tasaka M, Morita MT (2013) Mechanism of higher plant gravity sensing. *Am J Bot* 100:91–100.
54. Tasaka M, Kato T, Fukaki H (1999) The endodermis and shoot gravitropism. *Trends Plant Sci* 4:103–107.
55. Morita MT, et al. (2002) Involvement of the vacuoles of the endodermis in the early process of shoot gravitropism in *Arabidopsis*. *Plant Cell* 14:47–56.
56. Friml J, Wiśniewska J, Benková E, Mendgen K, Palme K (2002) Lateral relocation of auxin efflux regulator PIN3 mediates tropism in *Arabidopsis*. *Nature* 415:806–809.
57. Groover A (2016) Gravitropisms and reaction woods of forest trees—Evolution, functions and mechanisms. *New Phytol* 211:790–802.
58. Silady RA, et al. (2008) The GRV2/RME-8 protein of *Arabidopsis* functions in the late endocytic pathway and is required for vacuolar membrane flow. *Plant J* 53:29–41.
59. Silady RA, et al. (2004) The gravitropism defective 2 mutants of *Arabidopsis* are deficient in a protein implicated in endocytosis in *Caenorhabditis elegans*. *Plant Physiol* 136:3095–3103, discussion 3002.
60. Yano D, et al. (2003) A SNARE complex containing SGR3/AtVAM3 and ZIG/VTI11 in gravity-sensing cells is important for *Arabidopsis* shoot gravitropism. *Proc Natl Acad Sci USA* 100:8589–8594.
61. Tamura K, et al. (2007) *Arabidopsis* KAM2/GRV2 is required for proper endosome formation and functions in vacuolar sorting and determination of the embryo growth axis. *Plant Cell* 19:320–332.
62. Saito C, Morita MT, Kato T, Tasaka M (2005) Amyloplasts and vacuolar membrane dynamics in the living graviperceptive cell of the *Arabidopsis* inflorescence stem. *Plant Cell* 17:548–558.
63. Kato T, et al. (2002) SGR2, a phospholipase-like protein, and ZIG/SGR4, a SNARE, are involved in the shoot gravitropism of *Arabidopsis*. *Plant Cell* 14:33–46.
64. Guerriero G, Sergeant K, Hausman JF (2014) Wood biosynthesis and typologies: A molecular rhapsody. *Tree Physiol* 34:839–855.
65. Zhang J, Nieminen K, Serra JAA, Helariutta Y (2014) The formation of wood and its control. *Curr Opin Plant Biol* 17:56–63.
66. Barbez E, et al. (2012) A novel putative auxin Carrier family regulates intracellular auxin homeostasis in plants. *Nature* 485:119–122.
67. Spartz AK, et al. (2014) SAUR inhibition of PP2C-D phosphatases activates plasma membrane H+-ATPases to promote cell expansion in *Arabidopsis*. *Plant Cell* 26:2129–2142.
68. Schilling RK, Tester M, Marschner P, Plett DC, Roy SJ (2017) AVP1: One protein, many roles. *Trends Plant Sci* 22:154–162.
69. Ladwig F, et al. (2015) Phytosulfokine regulates growth in *Arabidopsis* through a response module at the plasma membrane that includes cyclic nucleotide-gated channel17, H^+-ATPase, and BAK1. *Plant Cell* 27:1718–1729.
70. Fuglsang AT, et al. (2014) Receptor kinase-mediated control of primary active proton pumping at the plasma membrane. *Plant J* 80:951–964.
71. Picco C, et al. (2015) Direct recording of trans-plasma membrane electron currents mediated by a member of the cytochrome b561 family of soybean. *Plant Physiol* 169:986–995.
72. Tabb A (2013) Shape from silhouette probability maps: Reconstruction of thin objects in the presence of silhouette extraction and calibration error. *Proceedings of the IEEE Computer Society Conference on Computer Vision and Pattern Recognition* (IEEE, New York), pp 161–168.
73. Tabb A (2014) Shape from inconsistent silhouette: Reconstructions of objects in the presence of segmentation and calibration error. PhD dissertation (Purdue University, West Lafayette, IN).
74. Tabb A, Park J (2015) Camera calibration correction in shape from inconsistent silhouette. *Proceedings of IEEE International Conference on Robotics and Automation* (IEEE, New York), pp 4827–4834.
75. Tabb A, Yousef KMA (2015) Parameterizations for reducing camera reprojection error for robot-world hand-eye calibration. *Proceedings of IEEE International Conference on Intelligent Robots and Systems* (IEEE, New York), pp 3030–3037.
76. Halir R, Flusser J (1998) Numerically stable direct least squares fitting of ellipses. *Proceedings of Sixth International Conference in Central Europe on Computer Graphics and Visualization. WSCG* (IEEE, New York), pp 125–132.
77. van Ooijen JW (2006) JoinMap 4.0: Software for the calculation of genetic linkage maps in experimental populations (Kyazma B.V., Wageningen, The Netherlands).
78. Kosambi DD (1943) The estimation of map distances from recombination values. *Ann Eugen* 12:172–175.
79. Voorrips RE (2002) MapChart: Software for the graphical presentation of linkage maps and QTLs. *J Hered* 93:77–78.
80. Edgar RC (2004) MUSCLE: Multiple sequence alignment with high accuracy and high throughput. *Nucleic Acids Res* 32:1792–1797.
81. Wang Z-P, et al. (2015) Egg cell-specific promoter-controlled CRISPR/Cas9 efficiently generates homozygous mutants for multiple target genes in *Arabidopsis* in a single generation. *Genome Biol* 16:144.
82. Mara C, Grigorova B, Liu Z (2010) Floral-dip transformation of *Arabidopsis thaliana* to examine pTSO2:beta-glucuronidase reporter gene expression. *J Vis Exp,* e1952.

PLANT BIOLOGY
Downloaded at Palestinian Territory, occupied on December 9, 2021
www.manaraa.com